

# Evaluation of Thumb-Operated Directional Pad Functionalities on a Glove-Based Optical Fiber Sensor

Eric Fujiwara, Yu Tzu Wu, Danilo Y. Miyatake, Murilo F. M. Santos, and Carlos K. Suzuki, *Member, IEEE*

**Abstract**—The implementation of directional pad functionalities on a glove-based optical fiber sensor by monitoring the thumb posture is reported. Multimode fiber bending transducers were attached to the glove to measure the flexion/extension and abduction/abduction movements of thumb joints. Then, the optical signals corresponding to each transducer were correlated to the relative finger position during the manipulation of a directional pad by using artificial neural networks. The estimation of thumb stationary location over the pad yielded a maximum absolute error of 4.3 mm, whereas the dynamic evaluation of finger trajectories resulted in errors lower than 5.5 mm. Furthermore, it was demonstrated that the glove sensor is able to identify the correct direction with 96.67% accuracy when applied as an eight-direction digital controller.

**Index Terms**—Data gloves, motion measurement, optical fiber application, optical fiber sensors, position measurement, user interfaces.

## I. INTRODUCTION

THE DEVELOPMENT of human–computer input interfacing technologies is primordial to the enhancement of collaborative working between user and systems, and to provide an immersive interaction with virtual or remote environments. In this sense, techniques based on the monitoring of hand movements are required to accomplish complex tasks with a precise, realistic, and intuitive approach. Examples of possible applications include teleoperation of robotic manipulators for exploring inhospitable or hazardous locations [1], robot-assisted surgeries [2], rehabilitation and therapy [3], virtual-reality systems [4], and interpretation of sign languages [5].

Currently, the investigation of hand posture can be performed by several techniques, such as optical tracking by external cameras [6], acoustic or magnetic tracking [7], electromyography [8], and glove-based sensors [9]. Among these methodologies, glove-based systems has exhibited notable characteristics, since they can provide a real-time and sensitive

Manuscript received September 10, 2012; revised November 8, 2012; accepted November 18, 2013. Date of publication May 16, 2013; date of current version July 10, 2013. This work was supported in part by FAPESP, CNPq/Universal, CNPq, and CAPES. The work of E. Fujiwara was supported by a scholarship from FAPESP. The Associate Editor coordinating the review process was Dr. Domenico Grimaldi.

The authors are with the Laboratory of Photonic Materials and Devices, State University of Campinas, Campinas, São Paulo 13083-970, Brazil (e-mail: fujiwara@fem.unicamp.br; wyutzu@gmail.com; danilo.miyatake@gmail.com; murilofms@fem.unicamp.br; suzuki@fem.unicamp.br).

Digital Object Identifier 10.1109/TIM.2013.2256817

response of the hand configuration, with a portable design and relative low cost, and are also not affected by latency or occlusion of fingers [9], [10].

Glove-based devices allow for direct measurement of the angular positions of hand joints by means of sensor arrays installed on the wearable support. Although a variety of transducers has been successfully demonstrated for monitoring the hand posture—including resistance-based flexsensors [11], [12], printable conductive mixtures [13], electroactive polymeric conductors [14], magnetic induction coils [15], electromagnetic sensors [16], [17], air pressure devices [18], and carbon nanotubes [19]—the utilization of optical fiber sensors is an attractive technology to be employed in glove-based devices, providing advantages in terms of performance and reliability due to their inherent characteristics, such as their light weight, flexibility, multiplexing capability, and immunity to electromagnetic interference [20]. Recent developments comprise the analysis of hand posture by measuring the bending losses on hetero-core structures [21] or flexible microbending transducers [22], and the spectral response of fiber Bragg gratings [23].

On the other hand, some tasks involving control of mobile robots, operation of user-interfaces, and video games can be executed more intuitively by mapping the commands to directional pad inputs, typically found in game controllers [24], [25]. Therefore, an interesting purpose would consist of integrating the functionalities of a directional pad to glove-based sensors, providing a versatile interface to the accomplishment of tasks that demand different approaches for the hand configuration.

In this context, present research reports a methodology to emulate the operation of a directional pad to the thumb by monitoring its movements using a glove-based optical fiber sensor. The correlation of the finger joint angles and the position in the pad coordinates system is performed by artificial neural networks algorithms, and the evaluation of the sensor response is demonstrated for both static and dynamic measurements.

## II. METHODOLOGY

### A. Hand Movements

The human hand is characterized as a complex mechanical system, constituted of bones and muscles connected by tendons and ligaments, and covered by a protective skin [26].

From the kinematics point of view, it can be described as a chain of links and rotational joints with one or more degrees of freedom (DOFs). In general, the whole hand is modeled according to  $\sim 21$  DOFs, but the calculations are facilitated by considering the natural constraints of movements [27].

The thumb posture is defined by the interphalangeal (IP), metacarpophalangeal (MP), and trapeziometacarpal (TP) joints, being comprised of one DOF for the IP, up to two DOFs for the MP, and up to three DOFs for the TP joint, depending on the adopted model [28]. During the manipulation of a digital controller, the user holds the device by adjusting his or her hand to the controller shape, and then operates the directional pad by positioning the thumb tip on desired direction and subsequently pressing or releasing the button. In this sense, the movements of the thumb on pad surface can be estimated by modeling the finger as a three DOFs system, in which one DOF is related to the IP, and two DOFs correspond to a combination of MP and TP joints. A representation of the thumb operation is illustrated in Fig. 1, where the kinematics of the finger is expressed according to the Denavit-Hartenberg (DH) convention, which allows determining the relative position and orientation of consecutive links [28]. The DH transformation matrix for the  $i$ th frame is given by

$${}_{i-1}A_i = \begin{bmatrix} \cos \theta_i & -\cos \alpha_i \sin \theta_i & \sin \alpha_i \sin \theta_i & a_i \cos \theta_i \\ \sin \theta_i & \cos \alpha_i \cos \theta_i & -\sin \alpha_i \cos \theta_i & a_i \sin \theta_i \\ 0 & \sin \alpha_i & \cos \alpha_i & d_i \\ 0 & 0 & 0 & 1 \end{bmatrix} \quad (1)$$

where  $\theta_i$  is the rotation in  $z$ -axis between the origin of coordinates systems for each joint,  $d_i$  and  $a_i$  are the distance of the coordinates systems in the  $x$ - and  $z$ -axis, respectively, and  $\alpha_i$  is the angular displacement in  $x$  between the joints. Therefore, for a manipulator formed by exclusively rotational joints,  $d_i$ ,  $a_i$  and  $\alpha_i$  are construction parameters, and the positions are expressed as a function of variable  $\theta_i$ . In case of the thumb movements, the angular position  $\theta_1$  is related to the abduction/adduction of the MP/TP joints, whereas  $\theta_2$  and  $\theta_3$  define the flexion/extension of the MP/TP and IP joints, respectively. Therefore, given the position of the thumb tip regarding to the coordinates system of the finger ( $x_0, y_0, z_0$ ), expressed by  $t$ , and the relative distance to the pad coordinates system ( $x_c, y_c, z_c$ ) given by  $r$ , the position  $s$  of the tip on the plane  $S$  referenced to the pad coordinates can be determined as a function of the hand, finger, and pad parameters.

### B. Glove-Based Sensor Design

The sensor consists of  $\sim 2$  m length standard silica multimode optical fibers with polymer buffer coating, in which a short segment of length  $L$  is attached to a textile glove. The glove is tightly adjusted to the user hand to avoid most of the wrinkles and slipping during the execution of movements, which could induce measurement errors. The fibers are fixed to the substrate by using an adhesive gel, periodically applied in positions  $d$  spaced by 5 mm, as shown in Fig. 2. Since the attached portions are located close to the IP, MP, and TP joints of the thumb (Fig. 3), as the finger is flexed, the fibers are bent and stresses are concentrated in the fixed positions due to the

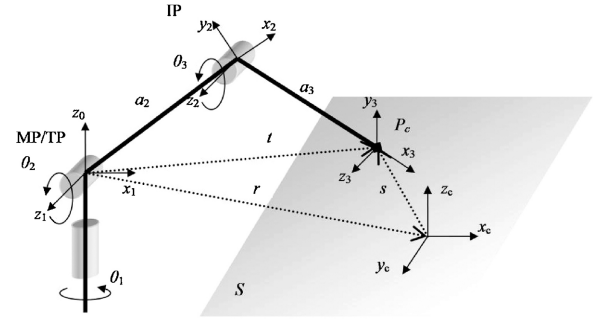


Fig. 1. Kinematics model and coordinates of the thumb-control pad system.

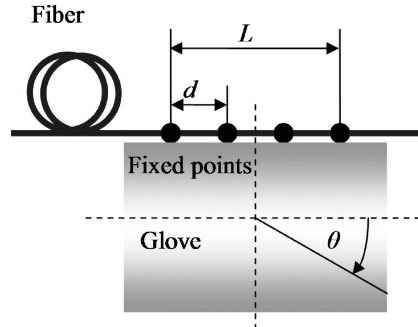


Fig. 2. Schematic of the fiber transducer.

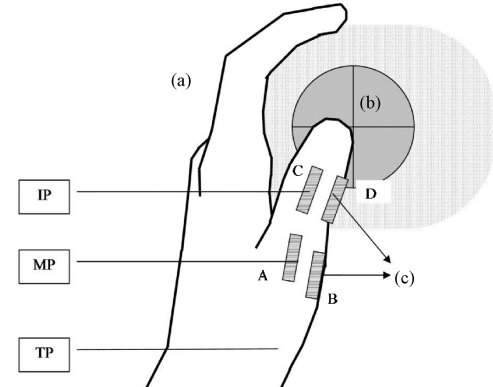


Fig. 3. User handling a control pad. (a) Glove (b) Pad. (c) Location of the attached fibers regarding the glove and pad.

differences on the mechanical properties of the fibers and the glove, causing attenuation of the transmitted light by bending losses. Therefore, the angular positions of the monitored joint can be correlated to the light intensities.

For the measurement of thumb movements, the optical fibers were placed in different locations of the finger, by attaching two fibers close to the IP joint, and two fibers in an intermediary position between the MP and TP joints, as summarized in Table I. In this sense, the glove sensor allows for detection of the flexion/extension movement of IP joint, as well as a combination of flexion/extension and abduction/adduction of the MP and TP joints.

### C. Experimental Setup

The experimental setup is presented in Fig. 4. Continuous white light emitted by a LED source is launched into the

TABLE I  
CONSTRUCTION PARAMETERS OF THE FIBER TRANSDUCERS

Configuration	Location	Length $L$ (mm)	Attached points
A	MP/TP, dorsal	40	9
B	MP/TP, lateral	20	5
C	IP, dorsal	25	6
D	IP, lateral	20	5

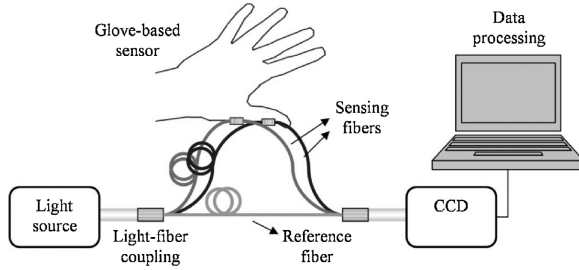


Fig. 4. Experimental setup of the sensor system.

multimode fibers, which are connected to the glove-based sensor. The output optical signal of each fiber is acquired by a CCD with a 10 Hz sampling rate, and then post-processed in the computer by using a software developed on the MATLAB environment. Furthermore, the stability of the source is monitored by a reference multimode fiber, which is kept apart of the glove, delivering the optical signal from the LED directly to the detector. In this sense, eventual fluctuations on source power are compensated by dividing light intensities from sensing fibers by the reference signal, and all analyses are carried out based on the normalized intensities.

### III. SENSOR CHARACTERIZATION

#### A. Characterization

In order to evaluate the sensor response as a controller, a  $50 \times 50 \times 20 \text{ mm}^3$  acrylic box was used as a dummy directional pad, by mapping the positions on the  $50 \times 50 \text{ mm}^2$  surface and defining the origin of the coordinates system at the center of the square, as shown in Fig. 5. Particularly, the dummy geometry was chosen because it anatomically fitted to the user hand, and its geometry resembles a commercial controller, making the operation of the sensor more intuitive.

The position of the finger tip  $P_c$  was varied according to the cylindrical coordinates  $(\rho, \varphi, z)$ , and the normalized intensity value for each fiber was calculated by considering a mean of 200 data points. For the sake of presentation, experimental data was adjusted by curve fitting. Regarding the displacement in  $z_c$  direction, the measurements were conducted by coupling a  $50 \times 50 \times 8 \text{ mm}^3$  structure on the dummy pad, which ensures that the increment in  $z$  was constant for all experiments. Moreover, during the measurements, the finger was kept on each position as stationary as possible, and the procedure was repeated several times to avoid variations on thumb tip position due to dithering or other physiological reasons, and to guarantee reliability of results.

The fiber output intensity curves exhibited characteristic patterns except by the configuration A (Fig. 6), related to the TM/TP joints, which was probably caused by the corrugation of the textile material during the extension of monitored

joints. On the other hand, the transducer setup B presented a good response to the combination of flexion/extension and abduction/adduction movements of TM and TP joints (Fig. 7) indicating that this configuration is less susceptible to the effects of glove deformation. Regarding the IP joint, both arrangements C and D generated suitable results, as shown in Figs. 8 and 9, respectively, with a higher sensitivity to the setup D, since the flexion produces a more acute fiber bending angle in case of placing the transducer on the lateral of finger. Moreover, it is also expected that the configuration D is less affected by the glove wrinkles during the extension movement.

As observed in Figs. 7 and 9, the variation on  $\varphi$  resulted in intensity curves with similar behaviors in terms of light attenuation for transducers B and D, which means that in general higher optical losses occur when the thumb tip is placed in quadrants QIII and QIV, which can be explained based on the flexion of finger joints and the relative positions of the thumb and pad coordinate systems origins,  $(x_0, y_0, z_0)$  and  $(x_c, y_c, z_c)$ , respectively. Due to the hand adjustment when the user manipulates the control pad, the TP joint, and consequently the origin of the thumb coordinates, is located in the quadrant QIII of the  $(x_c, y_c, z_c)$  system. In this sense, both IP and MP/TP joints present a maximum flexion for  $P_c$  values enclosed in QIII, as well as minimum flexions for positions in QI. This statement can be confirmed for configurations C and D, with the decrease of light attenuation for  $0^\circ < \varphi < 90^\circ$ , followed by the increase of optical losses for  $180^\circ < \varphi < 270^\circ$ , as a consequence of the higher bending angles. Alternatively, regarding the transducer B, the sensor response is also modulated by the abduction/adduction of the MP/TP joints, causing the minimum and maximum attenuation ranges to be shifted to quadrants QII and QIV, respectively, mostly because moving the finger toward the midline of the body implies on the increase of fiber bending.

Regarding  $\rho$  effects, the amplitude of the intensity curves increases for higher  $\rho$  values, once moving the finger tip to positions far from the origin of  $(x_c, y_c, z_c)$  system demands more intense angular displacements of the thumb joints, yielding to variations on the fiber bending conditions. However, it is also observed that transducers C and D have a little dependence with respect of  $\rho$  for  $\varphi$  values greater than  $180^\circ$ . This effect was generated because during the thumb tip operation on quadrants QIII and QIV, the variations on  $\rho$  are caused mostly in consequence of the adduction/abduction or flexing movements of the TP/MP joints, being slightly affected by the angular displacements of IP joint.

On the other hand, the dislocation along the  $z_c$ -axis resulted in a small shift on the intensity curves for lower  $\varphi$  values, which is most evidenced for the IP joint, as shown in Figs. 8 and 9. It occurs because a displacement  $z$  causes a constant increment in the flexion/extension angle of IP and MP/TP joints, inducing an off-set on the light intensity values, and this variation on the optical signal is expected to be more significant for higher  $z$  values.

#### B. Repeatability Analysis

In order to evaluate the repeatability of glove sensor, the transducers responses due to the operation by three different

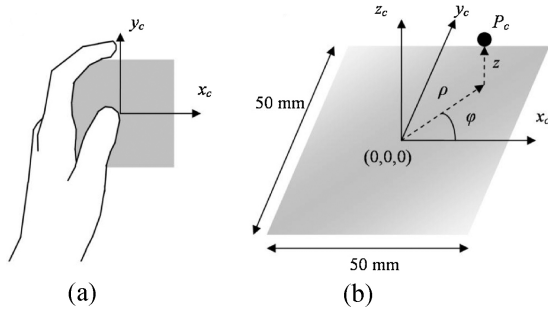


Fig. 5. Definition of the coordinates system of the control pad. (a) Hand position. (b) Position of the thumb tip  $P_c$ .

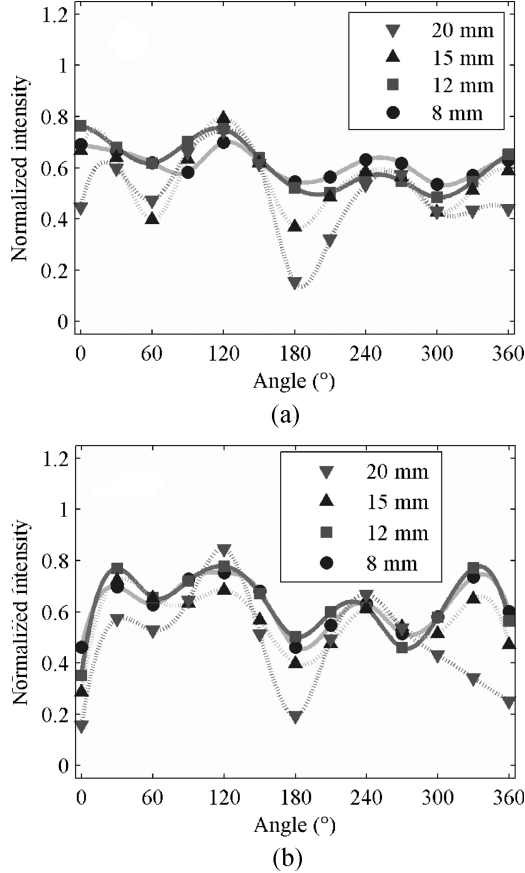


Fig. 6. Variation of normalized intensity for transducer A as a function of  $\varphi$  and  $\rho$ , for (a)  $z=0$  mm and (b)  $z=8$  mm. Experimental data fitted by smoothing spline.

users were analyzed. The experiment consisted alternately moving the thumb tip between positions  $\varphi=90^\circ$  and  $270^\circ$  for  $\rho=20$  mm, by maintaining the finger in each location for 5 s. An example is illustrated in Fig. 10, which demonstrates the normalized intensity signals of transducers B, C, and D for the pad handled by one of the subjects. The maximum and minimum intensity values correspond to the  $90^\circ$  and  $270^\circ$  positions, respectively, because the origin of thumb coordinates system is located in the quadrant QIII of pad coordinates, causing the IP and TP/MP joints to be flexed for  $\varphi=270^\circ$ , resulting in light attenuation by fiber bending, or extended for  $\varphi=90^\circ$ . The transducers C and D, applied on the monitoring of IP joint, presented a good repeatability, resulting

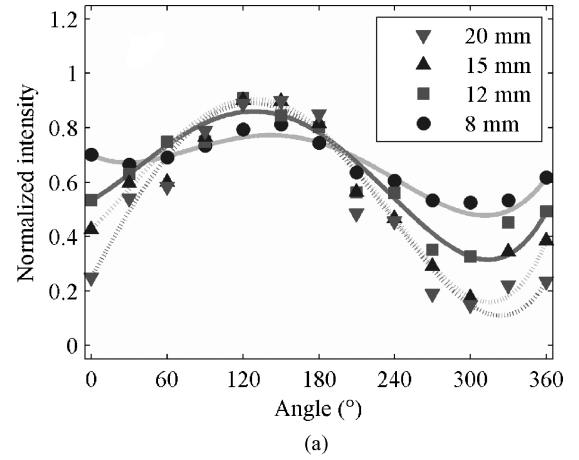


Fig. 7. Variation of normalized intensity for transducer B as a function of  $\varphi$  and  $\rho$ , for (a)  $z=0$  mm and (b)  $z=8$  mm. Experimental data fitted by 4<sup>th</sup> degree polynomial function.

in the same range of intensity values until the completion of the test. However, in case of transducer B, which was designed to measure the MP/TP joints, even though the optical signal levels were practically maintained during the measurements, variations on light intensities were observed probably due to the glove corrugation especially during the flexion movement.

Regarding the repeatability analysis for different users, Fig. 11 shows the normalized intensities obtained for  $90^\circ$  and  $270^\circ$  considering the average values of ten finger movement repetitions. The eventual variations on dynamic ranges for these positions were caused as a consequence of the differences on the dimensions of each subject hand, which affects the glove adjustment and relative location of transducers in respect to finger joints, as well as the handling of dummy pad. Concerning the deviations on intensity values, they were possibly caused due to errors generated by each subject on the finger positioning over the pad surface, since small variations on thumb tip location probably occurred during the position changes while the alternate movements were performed.

#### IV. MONITORING OF FINGER MOVEMENTS

##### A. Calibration and Validation

A software in MATLAB environment was developed for the tracking of finger tip on the pad surface. In this context, the

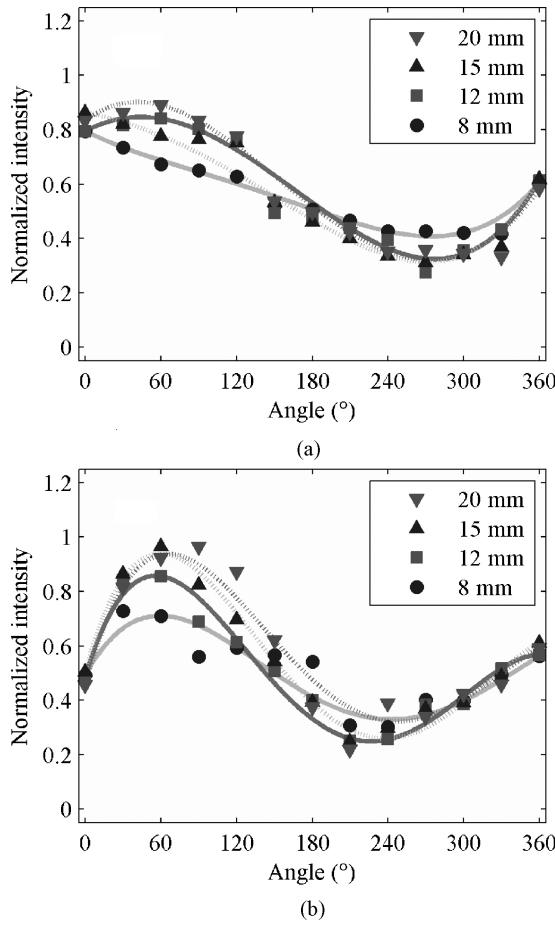


Fig. 8. Variation of normalized intensity for transducer C as a function of  $\varphi$  and  $\rho$ , for (a)  $z=0 \text{ mm}$  and (b)  $z=8 \text{ mm}$ . Experimental data fitted by 4<sup>th</sup> degree polynomial function.

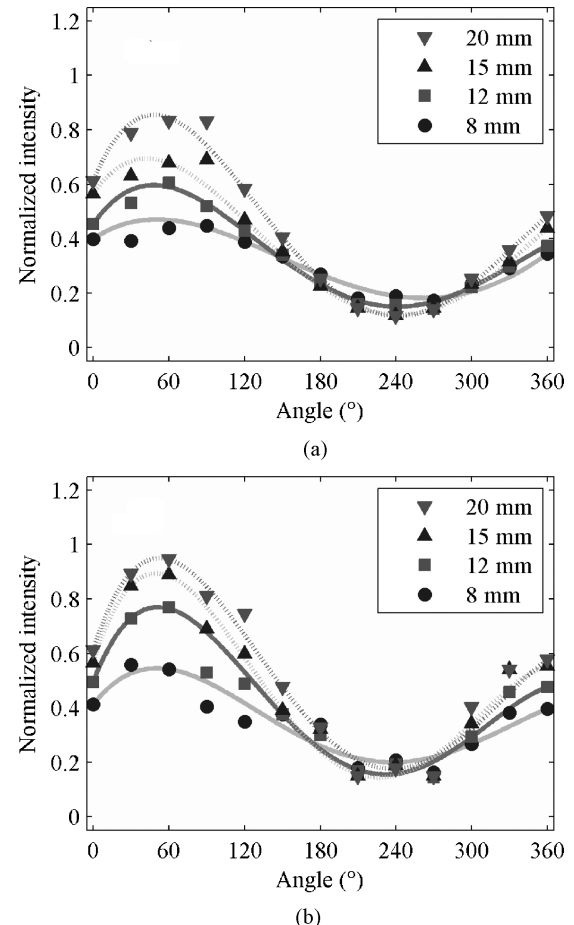


Fig. 9. Variation of normalized intensity for transducer D as a function of  $\varphi$  and  $\rho$ , for (a)  $z=0 \text{ mm}$  and (b)  $z=8 \text{ mm}$ . Experimental data fitted by 4<sup>th</sup> degree polynomial function.

correlation between light intensities and positions in  $(x_c, y_c, z_c)$  coordinates was performed by artificial neural networks (ANN). Initially, during the calibration procedure, the user was requested to place the thumb tip in defined locations of the pad, considering  $P_c$  values ranging from  $-20 \text{ mm}$  to  $20 \text{ mm}$  spaced by  $10 \text{ mm}$  in the  $x_c$  and  $y_c$  directions, and fixing the displacement  $z$  to 0. For each position, a dataset comprised by 100 normalized intensity values was obtained for the transducers B, C and D, being half of the records designated for the network training, whereas the remaining data was applied on the testing procedure. The ANN was designed according to the feed-forward backpropagation architecture [29] by addressing the light intensities to the input layer (100 neurons) and the positions in  $(x_c, y_c)$  axis to the output layer (two neurons). Additionally, four hidden layers (50 neurons) were implemented aiming the enhancement of network performance, and the transfer functions of input and hidden layers were set to the tangent sigmoidal, as the output layer was configured to the pure linear. Finally, the adjustment of weight matrix values was conducted using the scaled conjugated gradient backpropagation training function, and the network performance was verified on the evaluation of the remaining part of the dataset. The absolute error  $\Delta_{xy}$

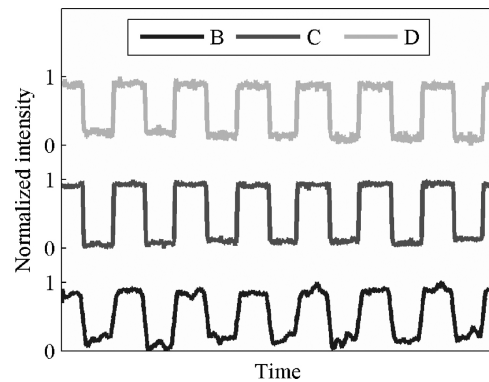


Fig. 10. Repeatability test of transducers B, C, and D for a single subject.

was calculated by

$$\Delta_{xy} = \sqrt{(x - x_n)^2 + (y - y_n)^2} \quad (2)$$

where  $(x_n, y_n)$  and  $(x, y)$  are the nominal and measured positions of the finger tip, respectively.

The results of the sensor validation are shown in Fig. 12. It is observed that the positions obtained by ANN computation are equivalent to the nominal ones, yielding to maximum and average absolute errors of 4.3 and 2.1 mm, respectively.

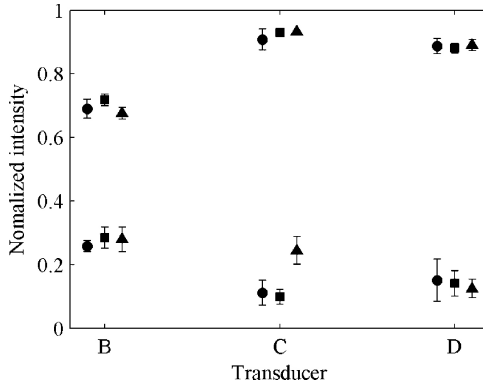


Fig. 11. Repeatability analysis for transducers B, C, and D, conducted by testing three different subjects (indicated by ●, ■, and ▲).

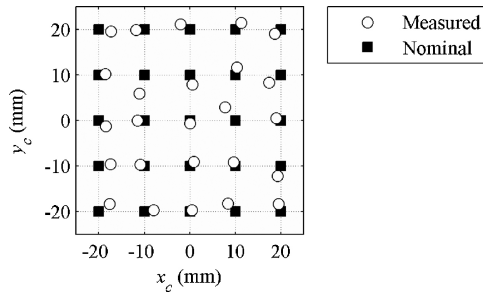


Fig. 12. Measurement error on the evaluation of the thumb tip position.

The eventual discrepancies between calculated and target data can be explained because the position of the thumb tip was assumed as a punctual value. However, during the handling of a controller, the user can press the directional pad with different parts of the frontal side of distal phalanx, suggesting that the practical position should be defined considering the contact area of the finger tip, this area being dependent on the anatomy of each user. For example, this effect can be also observed in Fig. 7, 8, and 9, which indicates that regarding the transducers B, C, and D, the same normalized intensity value was obtained for  $z=0$  mm and  $\varphi=210^\circ$ , if the parameter  $\rho$  is equal to 12 mm or 15 mm. In this case, both positions were probably enclosed in the same thumb area, yielding to errors during the calculation of finger location.

Regarding the time demanded for calibration procedure, given the 10 Hz sampling rate, the complete data acquisition demanded at least 125 s (25 positions and 50 intensity values for each point), considering that the total time also depends on the ANN training duration, which is determined by the network parameters and the computational capabilities. In this sense, two approaches were studied to abbreviate the calibration time: reducing the number of reference positions or minimizing the amount of acquired data in each point. For the first case, the same calibration procedure was applied, but the number of positions was changed from 25 to nine (by considering locations from -20 mm to 20 mm spaced by 20 mm), and later to five (by eliminating the diagonals). The second study was carried out by varying the amount of measured values, based on the analysis of 50, 25, 16 or 12 intensities data. As the training was accomplished, the networks were tested for

TABLE II  
EFFECT OF CALIBRATION PARAMETERS ON MEASUREMENT ERROR AND CALIBRATION TIME

Positions	Values	Average absolute error (mm)	Calibration time (s) <sup>a</sup>
5	50	7.4	25
9	50	5.1	45
25	50	2.1	125
25	25	3.3	62.5
25	16	3.5	40
25	12	3.8	30

<sup>a</sup>For 10 Hz sampling rate, without considering the time consumed by ANN training.

the same 50 values dataset, and the average absolute errors were calculated to compare the results. According to Table II, in spite of the reduction of demanded time, the average error increases significantly for fewer calibration positions. This observation was expected because the network testing was carried out considering locations that were not included in the training dataset. Even though the ANN presented a good generalization capability [30], the network did not properly evaluate the intermediary points of each quadrant especially in the five-positions case, which explains the higher errors for this configuration. On the other hand, reducing the amount of acquired values resulted in a moderate increase of the error, with a gain from two to four times on the calibration time, which demonstrates that this approach could be interesting to make the calibration procedure less tedious. Nevertheless, the sensor precision is expected to be enhanced with a more intensive calibration procedure.

#### B. Dynamic measurements

The sensor was also evaluated on the monitoring of the finger movements for a dynamic approach. In this case, the user moved the finger tip according to trajectories stipulated on the pad surface. Then, given the calibration previously obtained, the positions were calculated by addressing the measured normalized intensity values to the ANN. In the first experiment, the system was tested for a square-shaped trajectory, defined in  $(x_c, y_c)$  coordinates by the vertices (20, 20), (-20, 20), (-20, -20) and (20, -20). Subsequently, the finger was moved in a path delimited by a circle of radius 20 mm and center in (0, 0). In order to attenuate the effect of the optical noise, the positions were calculated by considering a mean of five intensity acquisitions for each fiber. A comparison of nominal and measured trajectories is illustrated in Figs. 13 and 14. The obtained values were compatible to the expected ones, with a maximum absolute error of 5.3 and 5.4 mm for the square and circular trajectories, respectively. However, the calibration was performed based on discrete positions, the methodology provided a good estimation of the intermediary values, which was possible due to the generalization capability of the ANN [30]. Regarding the measurement errors, the major deviations are credited to the variations on the contact area of the thumb to the pad surface, as previously mentioned, yielding to uncertainties on the exact position of the finger tip in reference to the  $(x_c, y_c, z_c)$  coordinates. As observed for both cases, the finger movements did not described a

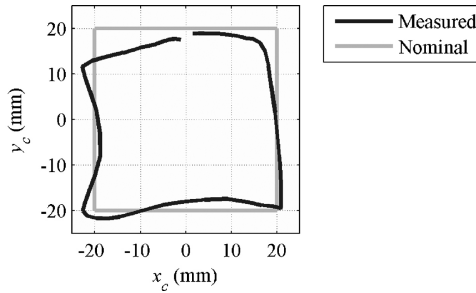


Fig. 13. Evaluation of the sensor response for a linear trajectory.

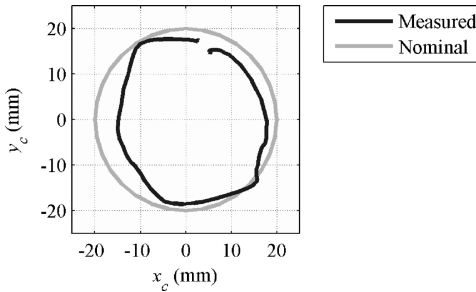


Fig. 14. Evaluation of the sensor response for a circular trajectory.

perfectly closed trajectory, which indicates that the initial and final positions are probably displaced as a consequence of the finger geometry. Another aspect is the error induced by user movements, since it is considerably difficult to draw a geometric figure with the thumb tip in a perfect trajectory.

## V. EVALUATION OF THE FIBER SENSOR AS A DIRECTIONAL PAD

The optical fiber sensor was also applied to perform the functionalities of a directional pad. Digital controllers are usually built with four electronic sensors, being each one of them responsible to receive the commands for a specific direction (up, down, left, and right), activated by a mechanical structure with cross geometry. Moreover, instructions regarding the movement to diagonal paths can be assigned by simultaneously actuating on adjacent directions, for example, exciting up and left transducers to generate the upper left position. Finally, due to mechanical constraints, opposite directions can not be pressed at the same time, which avoids command ambiguities.

The calibration was carried out by ANN according to the same setup of previous experiments, except by the output layer. In this case, the network was designed to return the positions relative to the vertical (down/up) and horizontal (left/right) directions with values ranging from -1 to 1, as shown in Table III, by using tangent sigmoidal transfer functions. Furthermore, a neutral condition was established for the situation in which both outputs are assigned with 0, indicating that not any direction was activated. The ANN processing was performed considering a 200 normalized intensity values dataset for each of nine possible positions for the pad (up, down, left, right, the four diagonals, and neutral), being half of the available data applied to the network training, and the remaining values used for testing the sensor performance. Since the directional pad

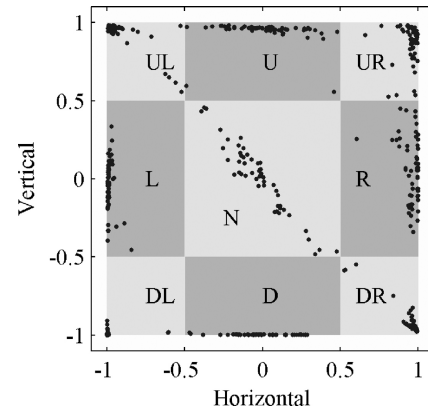


Fig. 15. Determination of the finger position according to the directional pad configuration. Experimental data was subsequently rounded to the nearest integer in order to stipulate the practical direction.

TABLE III  
EVALUATION OF THE FIBER SENSOR AS A DIRECTIONAL PAD

Direction	Vertical position	Horizontal position	Accuracy (%)
Neutral (N)	0	0	85.00
Right (R)	0	1	95.00
Upper right (UR)	1	1	98.33
Up (U)	1	0	95.00
Upper left (UL)	1	-1	100.00
Left (L)	0	-1	96.67
Lower left (DL)	-1	-1	100.00
Down (D)	-1	0	100.00
Lower right (DR)	-1	1	100.00

functionalities require the operation only on specific positions (-1, 0 or 1), the ANN output values were rounded to the nearest integer, and the selected direction was determined according to the combination of both output values.

As observed in Fig. 15 and summarized in Table III, the sensor was capable to identify the correct direction for 96.67% of the measurements, even considering the diagonal and neutral instances. Particularly, because this configuration is based in only nine defined directions, the sensor response is less affected by the thumb geometry, yielding to more precise detection. An alternative to improve the user interaction consists in emulating the procedure of pressing or releasing a button of the pad, which is possible by the monitoring of the finger position in the  $z_c$  axis. In this case, the direction should be validated only for  $z=0$ , whereas values  $z>0$  must be assumed as neutral positions, since the pad is virtually not pressed.

## VI. CONCLUSION

The operation of a virtual directional pad by using the thumb monitored by a glove-based fiber sensor was successfully demonstrated. With the measurement of the IP joint as well as a combination of the TP and MP joints, and the utilization of artificial neural networks for the data processing, it was possible to predict the position of the finger tip in the pad surface for both static and dynamic experiments. Moreover, the evaluation of the sensor system on the simulation of an eight-directions

digital controller was also presented, allowing the correct determination of the direction for ~97% of the experiments. On the other hand, further developments are still necessary to make the sensor response more precise and the calibration procedure less tedious. In addition, the prediction of the thumb tip position in  $z_c$  direction is still necessary for applications that require the simulation of press/release events. The results obtained by this research can be useful on the development of human input technologies for the operation of real and virtual systems, in a more intuitive and realistic way.

## REFERENCES

- [1] P. van der Smagt, M. Grebenstein, H. Urbanek, N. Flugge, M. Strohmayer, G. Stillfried, J. Parrish, and A. Gustus, "Robotics of human movements," *J. Physiol.-Paris*, vol. 103, nos. 3–5, pp. 119–132, May–Sep. 2009.
- [2] R. H. Taylor and D. Stoianovici, "Medical robotics in computer-integrated surgery," *IEEE Trans. Robot. Autom.*, vol. 19, no. 5, pp. 765–781, Oct. 2003.
- [3] H. I. Krebs, J. J. Palazzolo, L. Dipietro, M. Ferraro, J. Krol, K. Ranneckleiv, B. T. Volpe, and N. Hogan, "Rehabilitation robotics: Performance-based progressive robot-assisted therapy," *Auton. Robot.*, vol. 15, no. 1, pp. 7–20, Jul. 2003.
- [4] A. Jaimes and N. Sebe, "Multimodal human-computer interaction: A survey," *Comput. Vis. Image Und.*, vol. 108, nos. 1–2, pp. 116–134, Oct.–Nov. 2007.
- [5] Q. Munib, M. Habeeb, B. Takruri, and H. A. Al-Malik, "American sign language (ASL) recognition based on hough transform and neural networks," *Expert Syst. Appl.*, vol. 32, no. 1, pp. 24–37, Jan. 2007.
- [6] C.-S. Chua, H. Guan, and Y.-K. Ho, "Model-based 3-D hand posture estimation from a single 2-D image," *Image Vision Comput.*, vol. 20, no. 3, pp. 191–202, Mar. 2002.
- [7] D. J. Sturman and D. Zeltzer, "A survey of glove-based input," *IEEE Comput. Graph.*, vol. 14, no. 1, pp. 30–39, Jan. 1994.
- [8] O. Fukuda, T. Tsuji, M. Kaneko, and A. Otsuka, "A human-assisting manipulator teleoperated by EMG signals and arm motions," *IEEE Trans. Robot. Autom.*, vol. 19, no. 2, pp. 210–222, Apr. 2003.
- [9] L. Dipietro, A. M. Sabatini, and P. Dario, "A survey of glove-based systems and their applications," *IEEE Trans. Syst. Man Cybern. C*, vol. 38, no. 4, pp. 461–482, Jul. 2008.
- [10] H. Zhou and H. Hu, "Human motion tracking for rehabilitation: A survey," *Biomed. Signal Proces.*, vol. 3, no. 1, pp. 1–18, Jan. 2008.
- [11] K. N. Tarchanidis and J. Lygouras, "Data glove with a force sensor," *IEEE Trans. Instrum. Meas.*, vol. 52, no. 3, pp. 984–989, Jun. 2003.
- [12] G. Saggio, "Mechanical model of flex sensors used to sense finger movements," *Sensor. Actuat. A Phys.*, vol. 185, pp. 53–58, Oct. 2012.
- [13] F. Lorusso, E. P. Scilingo, M. Tesconi, A. Tognetti, and D. De Rossi, "Strain sensing fabric for hand posture and gesture monitoring," *IEEE Trans. Inf. Technol. B*, vol. 9, no. 3, pp. 372–381, Sep. 2005.
- [14] E. P. Scilingo, F. Lorusso, A. Mazzoldi, and D. de Rossi, "Strain-sensing fabrics for wearable kinaesthetic-like systems," *IEEE Sens. J.*, vol. 3, no. 4, pp. 460–467, Aug. 2003.
- [15] C.-S. Fahn and H. Sun, "Development of a data glove with reducing sensors based on magnetic induction," *IEEE Trans. Ind. Electron.*, vol. 52, no. 2, pp. 585–594, Apr. 2005.
- [16] Y. Su, C. R. Allen, D. Geng, D. Burn, U. Brechany, G. D. Bell, and R. Rowland, "3-D motion system ("data-gloves"): Application for Parkinson's disease," *IEEE Trans. Instrum. Meas.*, vol. 52, no. 3, pp. 662–674, Jun. 2003.
- [17] Y. Su, M. H. Fisher, A. Wolczowski, G. D. Bell, D. J. Burn, and R. X. Gao, "Toward an EMG-controlled prosthetic hand using a 3-D electromagnetic positioning system," *IEEE Trans. Instrum. Meas.*, vol. 56, no. 1, pp. 178–186, Feb. 2007.
- [18] N. Karlsson, B. Karlsson, and P. Wide, "A glove equipped with finger flexion sensors as a command generator used in a fuzzy control system," *IEEE Trans. Instrum. Meas.*, vol. 47, no. 5, pp. 1330–1334, Oct. 1998.
- [19] T. Yamada, Y. Hayamizu, Y. Yamamoto, Y. Yomogida, A. Izadi-Najafabadi, D. N. Futaba, and K. Hata, "A stretchable carbon nanotube strain sensor for human-motion detection," *Nat. Nanotechnol.*, vol. 6, no. 5, pp. 296–301, May 2011.
- [20] B. Culshaw, "Optical fiber sensor technologies: Opportunities and—perhaps—pitfalls," *J. Lightwave Technol.*, vol. 22, no. 1, pp. 39–50, Jan. 2004.
- [21] M. Nishiyama and K. Watanabe, "Wearable sensing glove with embedded hetero-core fiber-optic nerves for unconstrained hand motion capture," *IEEE Trans. Instrum. Meas.*, vol. 58, no. 12, pp. 3995–4000, Dec. 2009.
- [22] E. Fujiwara, Y. T. Wu, M. F. M. Santos, and C. K. Suzuki, "Development of an optical fiber transducer applied to the measurements of finger movements," in *Proc. SPIE OFS22*, vol. 8421. Beijing, China, 2012, pp. 8421H1–4.
- [23] A. F. S. Silva, A. F. Gonçalves, P. M. Mendes, and J. H. Correia, "FBG sensing glove for monitoring hand posture," *IEEE Sens. J.*, vol. 11, no. 10, pp. 2442–2448, Oct. 2011.
- [24] P. Rouanet, J. Bechu, and P.-Y. Oudeyer, "A comparison of three interfaces using handheld devices to intuitively drive and show objects to a social robot: The impact of underlying metaphors," in *Proc. IEEE RO-MAN*, Sep.–Oct. 2009, pp. 1066–1072.
- [25] G. Randelli, M. Venanzi, and D. Nardi, "Evaluating tangible paradigms for ground robot teleoperation," *Proc. IEEE RO-MAN*, 2011, pp. 389–394.
- [26] J. Lee and T. L. Kunii, "Model-based analysis of hand posture," *IEEE Comput. Graph.*, vol. 15, no. 5, pp. 77–86, Sep. 1995.
- [27] Y. Wu and T. S. Huang, "Hand modeling, analysis and recognition," *IEEE Signal Process. Mag.*, vol. 18, no. 3, pp. 51–60, May 2001.
- [28] B. Siciliano, L. Sciavicco, L. Vilani, and G. Oriolo, *Robotics: Modeling Planning and Control*. London, U.K.: Springer-Verlag, 2009, pp. 58–68.
- [29] H. Demuth and M. Beale, *Neural Network Toolbox for Use With MATLAB: User's Guide*. Natick, MA, USA: Mathworks, Inc., 2006, sec. 5.
- [30] I. A. Basheer and M. Hajmeer, "Artificial neural networks: Fundamentals, computing, design and application," *J. Microbiol. Meth.*, vol. 43, no. 1, pp. 3–31, Dec. 2000.

**Eric Fujiwara** was born in São Paulo, Brazil. He received the B.Sc. degree in control and automation engineering and the M.Sc. and Ph.D. degrees in mechanical engineering from the State University of Campinas (UNICAMP), Campinas, Brazil, in 2008, 2009, and 2012, respectively.

He joined the Laboratory of Photonic Materials and Devices, UNICAMP, in 2004, and has been involved with research and development of optical fiber sensors, automation, advanced optical materials, and fabrication of specialty fiber preforms.

**Yu Tzu Wu** was born in Taipei, Taiwan, China. She is currently an Undergraduate Student of control and automation engineering with the State University of Campinas (UNICAMP), Campinas, Brazil.

She joined the Laboratory of Photonic Materials and Devices, UNICAMP, in 2011 and has been involved with research and development of optical fiber sensors.

**Danilo Yugo Miyatake** was born in São Paulo, Brazil. He is currently an Undergraduate Student of control and automation engineering with the State University of Campinas (UNICAMP), Campinas, Brazil.

He joined the Laboratory of Photonic Materials and Devices, UNICAMP, in 2012 and has been involved with research and development of optical fiber sensors.

**Murilo Ferreira Marques dos Santos** was born in Rio Claro, Brazil. He received the B.Sc. degree in mechanical engineering from the State University of Campinas (UNICAMP), Campinas, Brazil, in 2011.

He joined the Laboratory of Photonic Materials and Devices, UNICAMP, in 2009, and has been involved with research and development of advanced optical materials and optical fiber sensors.

**Carlos Kenichi Suzuki** (M'11) was born in São Paulo, Brazil, on June 19, 1945. He received the B.S. and M.Sc. degrees in applied physics from São Paulo University, São Paulo, Brazil, and the State University of Campinas (UNICAMP), Campinas, Brazil, in 1969 and 1974, respectively, and the Dr. Eng. degree in applied physics engineering from the University of Tokyo, Tokyo, Japan, in 1981.

In 1982, he joined the Optical Fiber Project of Telebras-UNICAMP, where he was engaged in the development of optical fiber preform. From 1984 to 1990, he coordinated the international cooperation projects of JICA-UNICAMP and METI/ITIT-UNICAMP, developing highly perfect synthetic quartz and high-purity silica glass. From 1990 to 1993, he was a Research Fellow at the Spring-8 Laboratory, Harima, Japan. Since 1994, he has been a Professor of materials engineering in the area of new VAD technology at UNICAMP. He is an author of over 160 journal and conference papers. He holds 12 patents in Brazil and one PCT patent.

Dr. Suzuki is a member of the Brazilian Society of Materials Research.